Polymer 51 (2010) 5640–5648

Contents lists available at ScienceDirect

Polymer

journal homepage: www.elsevier.com/locate/polymer

Molecular simulations of neat, hydrated, and phosphoric acid-doped polybenzimidazoles. Part 1: Poly(2,2′-*m*-phenylene-5,5′-bibenzimidazole) (PBI), poly(2,5-benzimidazole) (ABPBI), and poly(*p*-phenylene benzobisimidazole) (PBDI)

Shuo Li [a], J.R. Fried [a,*], John Colebrook [b], Jonathan Burkhardt [a]

[a] Department of Chemical Engineering, University of Cincinnati, Cincinnati, OH 45221-0012, USA
[b] NSF REU student, Department of Chemical Engineering, Bucknell University, Lewisburg, PA 17837, USA

ARTICLE INFO

Article history:
Received 11 August 2010
Accepted 8 September 2010
Available online 17 September 2010

Keywords:
Polybenzimidazole
Phosphoric acid
Molecular simulation

ABSTRACT

Results of atomistic simulations of three polybenzimidazoles—poly(2,2′-*m*-phenylene-5,5′-bibenzimidazole) (PBI), poly(2,5-benzimidazole) (ABPBI), and poly(*p*-phenylene benzobisimidazole) (PBDI)—are reported in this communication. The effect of hydration and phosphoric acid (PA)-doping on the properties of these polybenzimidazoles have been studied. Densities and wide-angle X-ray diffraction (WAXD) patterns of the neat and PA-doped polybenzimidazoles agree well with available experimental results. Hydrogen bonding was examined in two ways. Radial distribution functions (RDFs) were used to measure bond lengths and the quantities of distinct types of bonds were counted. Both methods agree well with each other and indicate the strength of hydrogen bonding is mainly determined by the donor. Donor strength decreases in the order PA > water > polybenzimidazole. In the case that donors are the same, the hydroxyl oxygen atom in PA acting as acceptor forms the strongest hydrogen bond compared to other types of hydrogen acceptors. In addition, results suggest that PBI is less hydrophilic and has a lower affinity towards PA than either ABPBI or PBDI.

© 2010 Elsevier Ltd. All rights reserved.

1. Introduction

Polybenzimidazoles are linear aromatic polymers that exhibit excellent mechanical strength, thermal stability, and high resistance to acids, bases, and oxidative attack [1]. These properties have led to their use in a variety of applications ranging from fire-resistant materials to membranes [2]. In particular, acid-doped polybenzimidazoles have shown promise as proton-exchange membranes (PEMs) for fuel cell use at temperatures up to 200 °C. The most frequently used dopant is phosphoric acid (PA), introduced in 1995 by Wainright [3]. Compared with perfluorosulfonic acid PEMs, such as Nafion® [4], acid-doped polybenzimidazoles can maintain high proton conductivity at elevated temperatures (>100 °C) even at low water content [5–9]. In addition to the higher conductivity associated with higher temperatures, the use of high temperatures reduces poisoning of the catalyst by trace amounts of carbon monoxide [10,11]. Polybenzimidazoles are either amorphous [12], or exhibit low crystallity in fiber form as revealed by X-ray diffraction studies [13–21], and are hydrophilic [22–25]. As generally observed, the level of acid doping and water uptake are two critical factors that influence both conductivity and mechanical strength of the membrane. Ma et al. [26] have proposed a mechanism for proton transport in the polybenzimidazole–PA–water system based on experimental studies and have shown the importance of hydrogen bonding. While experimental values of membrane conductivity and the structural and mechanical properties of these systems are available in the literature, simulation studies have not been reported. This communication reports the first such study to explore hydrogen bonding in neat polybenzimidazoles as well as hydrated and PA-doped systems.

In this study, molecular dynamics (MD) is used to investigate hydrogen bonding in neat, hydrated, and PA-doped polybenzimidazoles. Polybenzimidazoles include poly(2,2′-*m*-phenylene-5,5′-bibenzimidazole) (PBI, Fig. 1A), poly(2,5-benzimidazole) (ABPBI, Fig. 1B), and poly(*p*-phenylene benzobisimidazole) (PBDI, Fig. 1C). PBI, with a reported glass transition temperature, T_g, of 420 °C [1], is the only commercially used polybenzimidazole and the majority of experimental studies have focused on acid-doped PBI membranes

* Corresponding author. Current address: Chemical and Materials Engineering, University of Dayton, Dayton OH 45469, USA. Tel.: +1 937 229 2670; fax: +1 937 229 3433.
E-mail address: jfried1@notes.udayton.edu (J.R. Fried).

0032-3861/$ – see front matter © 2010 Elsevier Ltd. All rights reserved.
doi:10.1016/j.polymer.2010.09.021

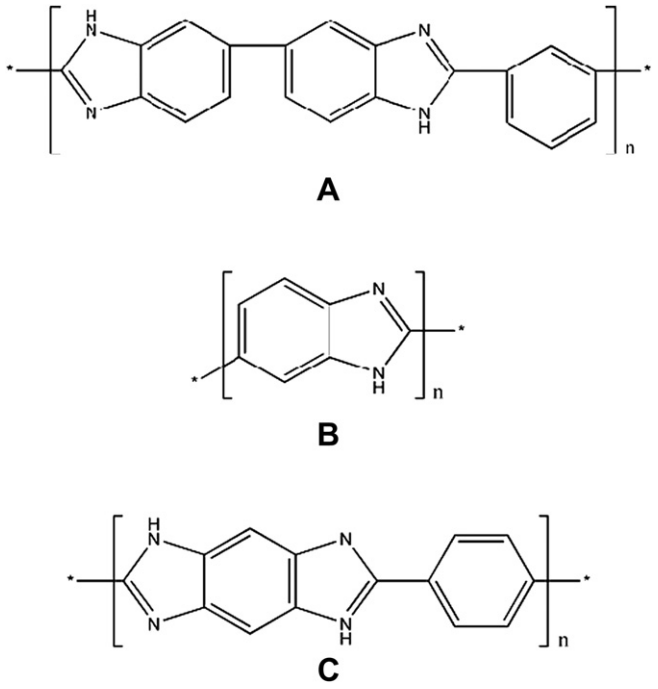

Fig. 1. Structures of (A) poly(2,2′-*m*-phenylene-5,5′-bibenzimidazole) (PBI), (B) poly (2,5-benzimidazole) (ABPBI), and (C) poly(*p*-phenylene benzobisimidazole) (PBDI).

[8,9]. ABPBI, which has a smaller repeat unit structure, has also been widely investigated for PEM applications [6,7]. Although PBDI has not been as widely studied, its crystalline and hydrated structures are available from published X-ray crystallography of a diimidazole model compound [25]. Besides, PBDI–water interactions reported in that study provides valuable insight into the behavior of solute molecules for both hydrated and acid-doped polybenzimidazole systems.

2. Computational methodology

2.1. Force field

The molecular mechanics force field used in this study is COMPASS (Condensed-phase Optimized Molecular Potentials for Atomistic Simulation Studies) [27,28] available through Materials Studio 5.0 [29]. COMPASS is a Class II *ab initio* force field that derives potential energy terms and some parameters from Consistent Force Field (CFF) [30,31] but uses condensed-phase data for final parameterization. As shown by Eq. (1), COMPASS utilizes quartic bond stretch (b) and angle-bend (θ) contributions, three-term cosine expansions for torsion (Φ), out-of-plane angle (χ), and a number of cross terms for coupled intramolecular interactions in the bonded potential. Non-bonded terms include a Coulombic potential and a 6–9L-J potential for van der Waals interaction [27].

2.2. Construction of amorphous cells

Single chains of each of the three benzimidazole polymers were built at random torsion angles from the POLYMERIZE_TAB in Materials Studio 5.0 [29]. To maintain comparable unit-cell dimensions, chain lengths consisted of 75, 100, and 200 repeat units (RUs) for PBI, PBDI, and ABPBI, respectively. Before using the AMORPHOUS_CELL module to build box around a polymer chain to represent the neat polybenzimidazole system, molecular mechanics using the COMPASS force field was performed through the FORCITE module to calculate average bond lengths and angles for the imidazole moiety and compare with available experimental results in the literature [25,32,33]. As shown in Table 1, the COMPASS values agree reasonably well with experimental results. Considering each imidazole moiety would allow a maximum of two attached water molecules [22–24], hydrated polybenzimidazole systems were constructed by mixing a polymer chain with sufficient water molecules to provide a 1:2 ratio of imidazole moieties to water molecules through the AMORPHOUS_CELL module. Similarly, the acid-doped systems were constructed by mixing a polymer chain with an appropriate numbers of PA and water molecules to form a 1:2:2 ratio of imidazole moieties to PA molecules to water molecules, referring to studies by Ma et al. [26] and Asensio et al. [20]. The initial target density of all amorphous cells was set as 1.4 g/cm^3. The option of ramp density from an initial value of 0.1 g/cm^3 was used to avoid cell generation failure due to the rigid structure of polybenzimidazoles. Each cell was followed by energy minimization using the "Smart" algorithm.

2.3. Molecular dynamics

To equilibrate these systems, 100-ps NVT dynamics was followed by 800-ps NPT dynamics using COMPASS through the FORCITE module. The time step for dynamics was 1 fs. The temperature was controlled at 298 K using the Andersen thermostat [34] and pressure was maintained around 1 atm using the Berendsen barostat [35]. Ewald summation [36] was utilized for both van der Waals and Coulombic interactions. Except for periodic boundary conditions, there were no additional symmetry constraints.

Cell density, wide-angle X-ray diffraction (WAXD) patterns, radial distribution functions (RDFs), and the numbers of distinct hydrogen bonds were calculated for all systems using the last 200 ps of NPT dynamics. WAXD patterns were used to calculate the intersegmental or d-spacing using the Bragg equation

$$d = \frac{\lambda}{2\sin\theta} \tag{2}$$

where λ is the wavelength (1.54 Å for Cu Kα radiation) and θ is the scattering angle corresponding to the maximum of the principal peak in a plot of intensity versus the scattering angle, 2θ. RDFs were used to estimate lengths of different types of hydrogen bonds and distances between hydrogen donor and acceptor atoms. The RDF for an atom pair of A and B, $g_{AB}(r)$, gives the probability of finding B

$$\begin{aligned}
E_{total} &= E_b + E_\theta + E_\phi + E_\chi + E_{bb'} + E_{b\theta} + E_{b\phi} + E_{\theta\phi} + E_{\theta\theta'} + E_{\theta\theta'\phi} + E_{elec} + E_{LJ} \\
&= \sum_b \left[K_2(b-b_o)^2 + K_3(b-b_o)^3 + K_4(b-b_o)^4\right] + \sum_\theta \left[H_2(\theta-\theta_o)^2 + H_3(\theta-\theta_o)^3 + H_4(\theta-\theta_o)^4\right] \\
&+ \sum_\phi [V_1(1-\cos\phi) + V_2(1-\cos 2\phi) + V_3(1-\cos 3\phi)] + \sum_\chi K_\chi(\chi-\chi_o)^2 + \sum_{b,b'} F_{b,b'}(b-b_o)\left(b'-b'_o\right) + \sum_{b,\theta} F_{b,\theta}(b-b_o)(\theta-\theta_o) \\
&+ \sum_{b,\phi}(b-b_o)\left[F^{(1)}_{b,\phi}\cos\phi + F^{(2)}_{b,\phi}\cos 2\phi + F^{(3)}_{b,\phi}\cos 3\phi\right] + \sum_{\theta,\phi}(\theta-\theta_o)\left[F^{(1)}_{\theta,\phi}\cos\phi + F^{(2)}_{\theta,\phi}\cos 2\phi + F^{(3)}_{\theta,\phi}\cos 3\phi\right] \\
&+ \sum_{\theta\theta'} F_{\theta,\theta'}(\theta-\theta_o)\left(\theta'-\theta'_o\right) + \sum_{\theta,\theta',\phi} F_{\theta,\theta',\phi}(\theta-\theta_o)\left(\theta'-\theta'_o\right)\cos(\phi-\phi_o) + \sum_{i,j}\frac{q_i q_j}{r_{ij}} + \sum_{i,j}\varepsilon_{ij}\left[2\left(\frac{r^o_{ij}}{r_{ij}}\right)^9 - 3\left(\frac{r^o_{ij}}{r_{ij}}\right)^6\right].
\end{aligned} \tag{1}$$

Table 1
Selected ring dimensions for the imidazole moiety in PBI, ABPBI, and PBDI.

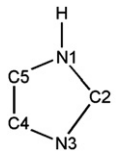

Numbering scheme

	PBI	ABPBI	PBDI	Imidazole (exp.)[a]	Benzimidazole (exp.)[b]	2,6-Diphenyl(1,2-d;5,4-d′) benzodiimidazole (exp.)[c]
N1–H (Å)	0.993	0.994	0.995	–	–	–
N1–C2 (Å)	1.339	1.339	1.339	1.311	1.311	1.356
C2–N3 (Å)	1.357	1.361	1.358	1.337	1.346	1.333
N3–C4 (Å)	1.372	1.365	1.368	1.372	–	1.399
C4–C5 (Å)	1.376	1.376	1.389	1.311	–	1.425
C5–N1 (Å)	1.382	1.387	1.380	1.381	–	1.379
C–N1–C (°)	107.6	107.4	107.5	–	106.6	109.2
C–N3–C (°)	104.8	104.6	104.6	–	104.2	106

[a] Experimental values for imidazole, Ref. [32].
[b] Experimental values for benzimidazole, Ref. [33].
[c] Experimental values for 2,6-diphenyl(1,2-d;5,4-d′)benzodiimidazole, Ref [25]. Bond lengths and angles for some other benzimidazoles were summarized in this reference.

separated from A by a distance of r. From the dynamics trajectory it can be evaluated as

$$g_{AB}(r) = \frac{N_{AB}(r) \times V}{N_A N_B 4\pi r^2 dr} \quad (3)$$

where V is the volume of the cell, $N_{AB}(r)$ is the number of atoms of type B in the spherical shell around A from radius r to $r + dr$, N_A is the total number of atoms of type A in the cell, and N_B is the total number of type B. A Perl script was written to calculate the numbers of distinct hydrogen bonds over the last 200 ps of the NPT dynamics based on simple geometric criteria. Specifically, hydrogen donor and acceptor atoms must be within the cutoff distance of 2.5 Å and the angle formed by the donor, hydrogen, and acceptor atoms must be larger than 90 degrees to qualify as a hydrogen bond.

3. Results and discussions

3.1. Density

Dimensions of the amorphous cell and densities of neat, hydrated, and PA-doped polybenzimidazoles obtained from NPT simulations are summarized in Table 2. At the end of 800-ps NPT dynamics, the side lengths of the neat, hydrated, and PA-doped polybenzimidazole amorphous cells ranged from 31.9 Å to 41.4 Å. Densities of neat polybenzimidazoles were 1.173 g/cm^3 for both PBI and ABPBI and 1.178 g/cm^3 for PBDI. The density of PBI agrees well with the experimental value of untreated PBI fiber, 1.2 g/cm^3 [1,2]. Densities of annealed and plasticized [37] PBI fibers have been reported to be 1.3 g/cm^3 and 1.4 g/cm^3 [1,2]. The experimental density of ABPBI has been reported to be 1.4–1.6 g/cm^3 [38]. These higher densities may be attributed to the post-treatments that refine the polybenzimidazole structures by making them homogeneous and compact. For the three hydrated systems, hydrated ABPBI has the largest density at 1.259 g/cm^3 followed closely by a density of 1.253 g/cm^3 for hydrated PBDI. Hydrated PBI shows the lowest density value of 1.231 g/cm^3. Because water molecules can form hydrogen bonds with benzimidazole chains and fill the interchain space, the lower density of PBI suggests a lower hydrophilicity compared to both ABPBI and PBDI. This can be due to the extra hydrophobic phenyl ring in the PBI repeat unit, as shown in Fig. 1(A). This agrees with experimental data that PBI can absorb 15–19 wt.% water [22,23] and the water uptake by ABPBI is slightly higher than that of PBI [24]. Simulated densities of the PA-doped ABPBI, PBDI, and PBI were 1.650 g/cm^3, 1.640 g/cm^3, and 1.567 g/cm^3, respectively, which is consistent with the density trend for the hydrated systems.

Table 2
Dimensions of amorphous cell and densities of neat, hydrated, and PA-doped polybenzimidazoles obtained from NPT simulations.

	Number of atoms	Initial cell length (Å)	Final cell length (Å)	Final density (g/cm^3)	Standard deviation[a]
Neat PBI[b]	2702	30.16	31.93	1.173	0.006
Neat ABPBI[c]	2602	30.20	32.05	1.173	0.006
Neat PBDI	2602	30.20	31.95	1.178	0.005
Hydrated PBI	3602	32.34	33.82	1.231	0.004
Hydrated ABPBI	3802	33.05	34.34	1.259	0.004
Hydrated PBDI	3802	33.05	34.31	1.253	0.006
PA-doped PBI	6002	40.95	39.48	1.567	0.004
PA-doped ABPBI	7002	43.54	41.19	1.650	0.005
PA-doped PBDI	7002	43.54	41.35	1.640	0.007

[a] Standard deviation of average value over the last 200 ps of NPT dynamics.
[b] The experimental density of untreated PBI is 1.2 g/cm^3, and densities of annealed and plasticized PBI fibers have been reported to be 1.3 g/cm^3 and 1.4 g/cm^3, Ref. [1, 2].
[c] The experimental density of ABPBI has been reported to be 1.4–1.6 g/cm^3, Ref. [38].

3.2. WAXD

Diffraction patterns of neat, hydrated, and PA-doped polybenzimidazoles obtained from NPT simulations are shown in Fig. 2. As shown, a single broad peak exists for each polybenzimidazole. The scattering angle, 2θ, corresponding to the maximum of the peak, is nearly the same for all three polybenzimidazoles but is shifted depending on whether the polymer is hydrated or PA-doped. For neat PBI, ABPBI, and PBDI, 2θ is 16.7°, 16.8°, and 16.0°, respectively. The corresponding d-spacing, calculated from Eq. (2), lies in the range from 5.3 to 5.5 Å, in reasonable agreement with the experimental results of Inoue et al. [12]. They have reported a d-spacing of 4.7 Å for amorphous PBI powders. Experimental WAXD patterns also have been reported for partially crystalline polybenzimidazoles. These usually have the same shape as the simulated spectra but exhibit a d-spacing of 3.4 Å [13–16], attributed to the spacing between two parallel benzimidazole chains. The small shift of our simulated WAXD patterns from these experimental patterns is consistent with the density results. As explained in Section 3.1, post-treatment processes for amorphous polybenzimidazoles refine their

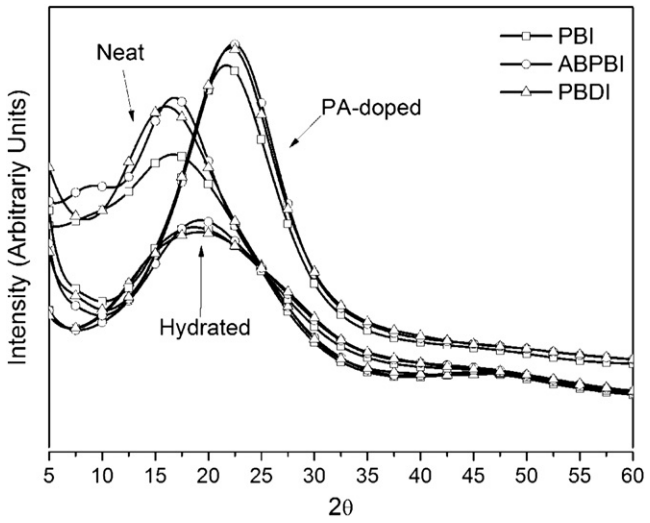

Fig. 2. WAXD patterns of neat, hydrated, and PA-doped PBI, ABPBI, and PBDI obtained from NPT simulations.

structures by making them less ordered and resulting in a low crystalline content. Crystallinity of PBI fibers has been reported to decrease under thermal treatment at 475 °C with *d*-spacing increasing from 3.4 Å to 4.4 Å [19]. For the hydrated systems, 2θ is 18.7° for hydrated PBI and 19.2° for hydrated ABPBI and PBDI, corresponding to a *d*-spacing of 4.7 Å. The corresponding scattering angles (2θ) for acid-doped PBI, ABPBI, and PBDI are 21.7°, 22.4°, and 22.1° (*d*-spacing ~4.0 Å). This agrees very well with the experimental results of Asensio et al. [20,21]. According to their study, the *d*-spacing for partially crystalline ABPBI fibers increased from 3.4 Å to 4.0 Å as the PA-doping level (number of PA molecules/number of RUs) increases from 0 to 3. When polybenzimidazole is doped with PA, the residual crystalline order is completely lost due to the plasticization. This also corresponds to a significant decrease in T_g observed by Hughes et al. [39] using differential scanning calorimetry. The good agreement between simulation and experimental results for PA-doped systems is of high importance considering their fuel cell applications. In contrast with the trend that Asensio et al. reported [20,21], simulation results show the *d*-spacing of polybenzimidazoles decreases as water and PA were added. This difference has been attributed to the fully amorphous model used in this simulation study. The decreased interchain spacing is probably due to hydrogen bonding between water and PA and the benzimidazole chain. Compared to water, PA molecules can form stronger hydrogen bonds with the benzimidazole chain, as shown by results presented in the following sections.

3.3. RDF

Table 3 lists the atom typing in COMPASS for benzimidazole, water, and PA. RDF plots for twelve atom pairs involved in hydrogen bonding in neat, hydrated, and PA-doped polybenzimidazoles are shown in Figs. 3–6. Results indicate that calculated lengths of hydrogen bonds and distances between hydrogen donor and acceptor atoms are comparable for all three polybenzimidazoles. To make RDF results easier to interpret, schematic representations of hydrogen bonding in neat, hydrated, and PA-doped polybenzimidazoles are illustrated in Fig. 7. Detailed descriptions of the RDF results follow.

Fig. 3 shows RDF plots for the "n3a–h1n ⋯ n2a" hydrogen bonding in the three neat polybenzimidazoles. For all three, the peak of $g_{n3a-n2a}(r)$ at $r = 3.0$ Å corresponds to the hydrogen bonding of "n3a–h1n ⋯ n2a" between parallel imidazole rings. The peak of $g_{h1n-n2a}(r)$ at $r = 2.0$ Å corresponds to the bond length.

Fig. 4 shows RDF plots for three types of intermolecular hydrogen bonding in hydrated polybenzimidazoles. The peak of $g_{n3a-o2^*}(r)$ at $r = 3.0$ Å describes the correlation between "n3a" and "o2*"atoms representing hydrogen bonding involving "n3a–h1n ⋯ o2*". The length of this hydrogen bond is 2.0 Å, as shown by $g_{h1n-o2^*}(r)$. The peak of $g_{o2^*-n2a}(r)$ at $r = 2.8$ Å describes the correlation between "o2*" and "n2a" representing hydrogen bonding involving "o2*–h1o ⋯ n2a". The length of this hydrogen bond is 1.8 Å, as shown by $g_{h1o-n2a}(r)$. In addition, RDFs of $g_{o2^*-o2^*}(r)$ and $g_{h1o-o2^*}(r)$ for hydrogen bonding between water molecules are shown in Fig. 4. The length of this hydrogen bond is 1.8 Å with a O–O distance of 2.8 Å. These results agree reasonable well with experimental results (1.85 Å for H–O and 2.88 Å for O–O distances) [40] and TIP3P (2.77 Å for H–O and 1.83 Å for O–O distances) and SPC (1.80 Å for H–O and 2.78 Å for O–O distances) water models [41]. RDFs for the "n3a–h1n ⋯ n2a" hydrogen bond in hydrated polybenzimidazoles are consistent with those in neat polybenzimidazoles, as shown in Fig. 3.

Table 3
Atom typing in COMPASS for benzimidazole, water, and PA.

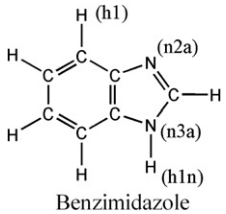

Benzimidazole

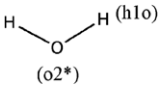

Water

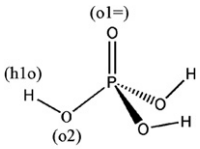

PA

Molecule	Atom	Atom assignment	Description	Role in hydrogen bonding
Benzimidazole	N	n2a	Nitrogen, SP2, 2 partial double bonds	Acceptor
	N	n3a	Nitrogen, SP2	Donor
	H	h1n	Hydrogen bound to nitrogen	Hydrogen
	H	h1	Hydrogen bound to carbon	–
Water	O	o2*	Oxygen, SP3, in water	Donor and acceptor
	H	h1o	Hydrogen bound to oxygen	Hydrogen
PA	O	o1=	Oxygen, SP2, double bound to phosphorus	Acceptor
	O	o2	Oxygen, SP3, generic	Donor and acceptor
	H	h1o	Hydrogen bound to oxygen	Hydrogen

Therefore, they are not repeated in Fig. 4 but are included in Supporting Information instead.

Fig. 5 shows RDF plots for three types of intermolecular hydrogen bonding between polybenzimidazole and PA molecules in PA-doped polybenzimidazoles. As shown, the hydrogen bond of "n3a–h1n ⋯ o1=" has a length of 2.0 Å, with a distance of 3.0 Å between "n3a" and "o1=". The length of the "n3a–h1n ⋯ o2" hydrogen bond is around 1.9 Å, with a broad distribution in the range of 2.8 Å and 3.0 Å for "n3a–o2" correlations. The length of the "o2–h1o ⋯ n2a" hydrogen bond is 1.7 Å, with a distance of 2.6 Å between "o2" and "n2a".

In Fig. 6, RDF plots are shown for different types of hydrogen bonding between PA and water molecules in PA-doped polybenzimidazoles. Our earlier RDF study on neat PA showed the two types of hydrogen bonds between PA molecules, "o2–h1o⋯ o2" and "o2–h1o ⋯ o1=", with lengths of 1.5 Å and 1.7 Å, respectively [42]. In this study, the distance of "o2–o2" is calculated to be in the range of 2.7 Å and 2.9 Å and the distance of "o2–o1=" is calculated to be 2.4 Å, which agree well with RDF results for neat PA [42]. The lengths of three hydrogen bonds between PA and water molecules, "o2*–h1o ⋯ o1=", "o2*–h1o ⋯ o2", and "o2–h1o ⋯ o2*", are calculated to be 1.8 Å, 1.7 Å, and 1.7 Å, respectively. RDF plots for "o2*–o1=" and "o2–o2*" correlations show peaks near $r = 3.1$ Å and $r = 2.6$ Å, respectively. In addition, RDFs for hydrogen bonding of "n3a–h1n ⋯ n2a", "n3a–h1n ⋯ o2*", "o2*–h1o ⋯ n2a", and "o2*–h1o ⋯ o2*" in PA-doped polybenzimidazoles are consistent with those in neat and hydrated systems and are presented in Supporting Information.

The length of a hydrogen bond depends on the bond strength, and generally, a stronger hydrogen bond has a shorter length. Therefore, the order of the bond strength can be roughly estimated by comparing the lengths of different types of hydrogen bonds. In descending order, hydrogen bonding strength is: "o2–h1o⋯ o2" (1.5 Å, PA–PA) > "o2–h1o ⋯ o1=" (1.7 Å, PA–PA), "o2–h1o ⋯ o2*" (1.7 Å, PA–water), "o2–h1o ⋯ n2a" (1.7 Å, PA–benzimidazole), and "o2*–h1o ⋯ o2" (1.7 Å, water–PA) > "o2*–h1o ⋯ o1=" (1.8 Å, water–PA), "o2*–h1o⋯ o2*" (1.8 Å, water–water), and "o2*–h1o ⋯ n2a" (1.8 Å, water–benzimidazole) > "n3a–h1n ⋯ o2" (1.9 Å, benzimidazole–PA) > "n3a–h1n ⋯ o1="(2.0 Å, benzimidazole–PA), "n3a–h1n ⋯ o2*" (2.0 Å, benzimidazole–water), and "n3a–h1n ⋯ n2a" (2.0 Å, benzimidazole–benzimidazole). As shown, the hydroxyl oxygen atom, "o2", in PA can act as both hydrogen donor and acceptor. The other type of oxygen atoms, "o1=", in PA can be hydrogen acceptor only. Therefore, there are three types of hydrogen donors and four types of acceptors in total. Results show the strength of hydrogen bonding involved in this study is mainly determined by the donor and suggest the following trend of decreasing strength of hydrogen bonding: PA as donor > water as donor > polybenzimidazole as donor. In the case that donors are the same, the hydroxyl oxygen atom "o2" in PA, acting as acceptor, forms the strongest hydrogen bond compared to other acceptor atoms.

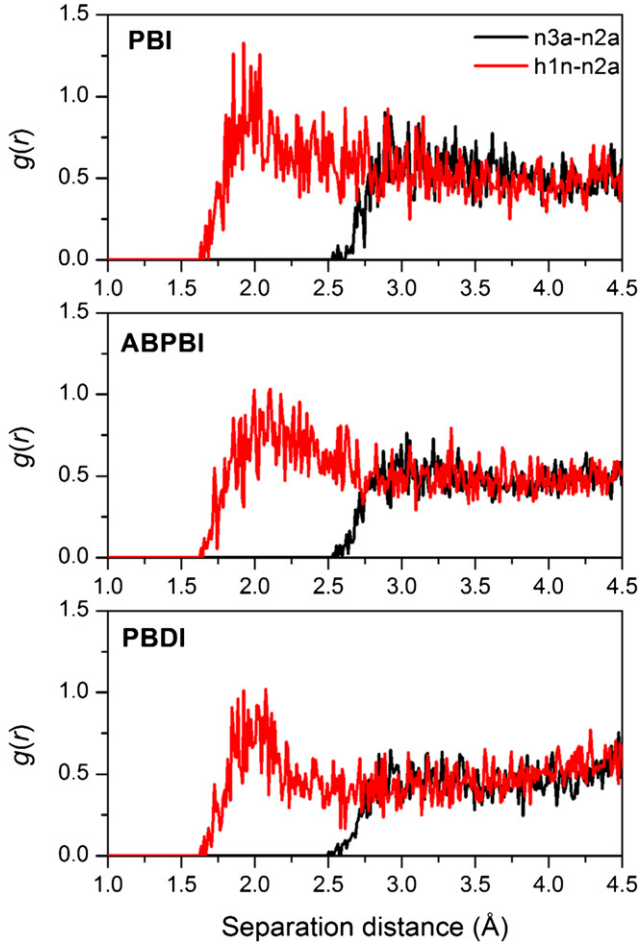

Fig. 3. RDF plots for intermolecular "n3a–n2a" and "h1n–n2a" atom pairs in neat PBI, ABPBI, and PBDI.

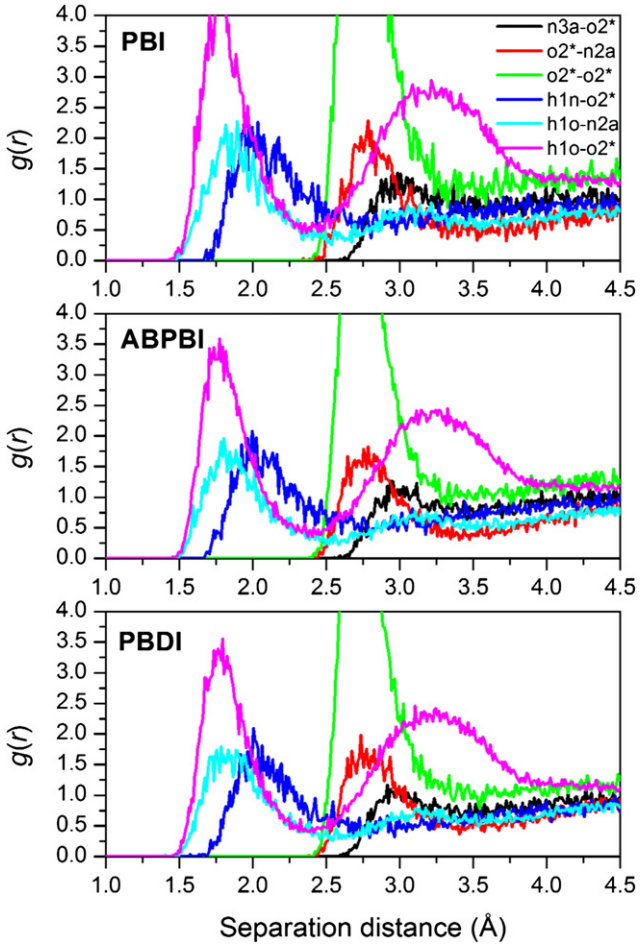

Fig. 4. RDF plots for intermolecular "n3a–o2*", "o2*–n2a", "o2*–o2*", "h1n–o2*", "h1o–n2a", and "h1o– o2*" atom pairs in hydrated PBI, ABPBI, and PBDI.

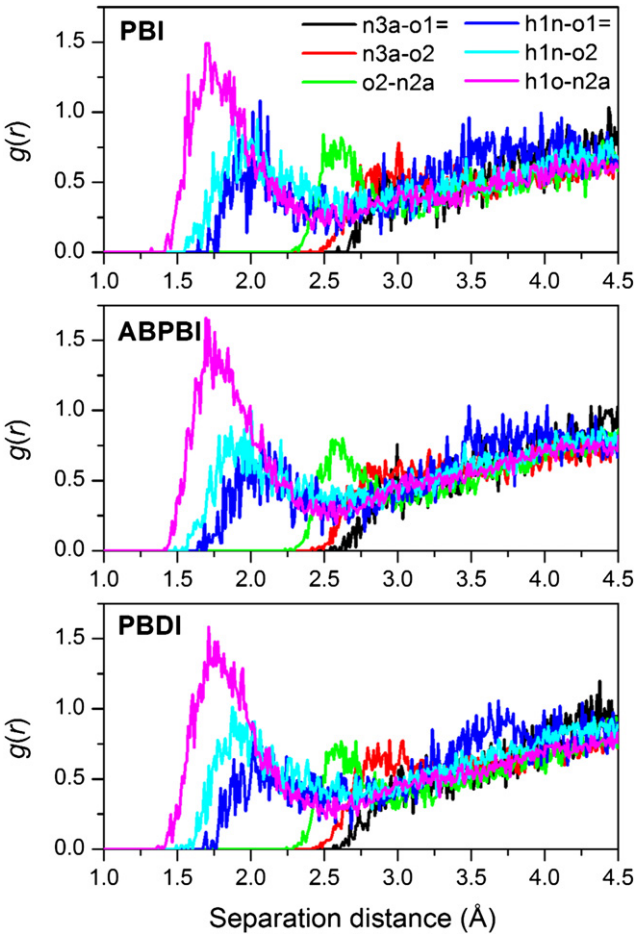

Fig. 5. RDF plots for intermolecular "n3a–o1=", "n3a–o2", "o2–n2a", "h1n–o1=", "h1n–o2", and "h1o–n2a" atom pairs in PA-doped PBI, ABPBI, and PBDI.

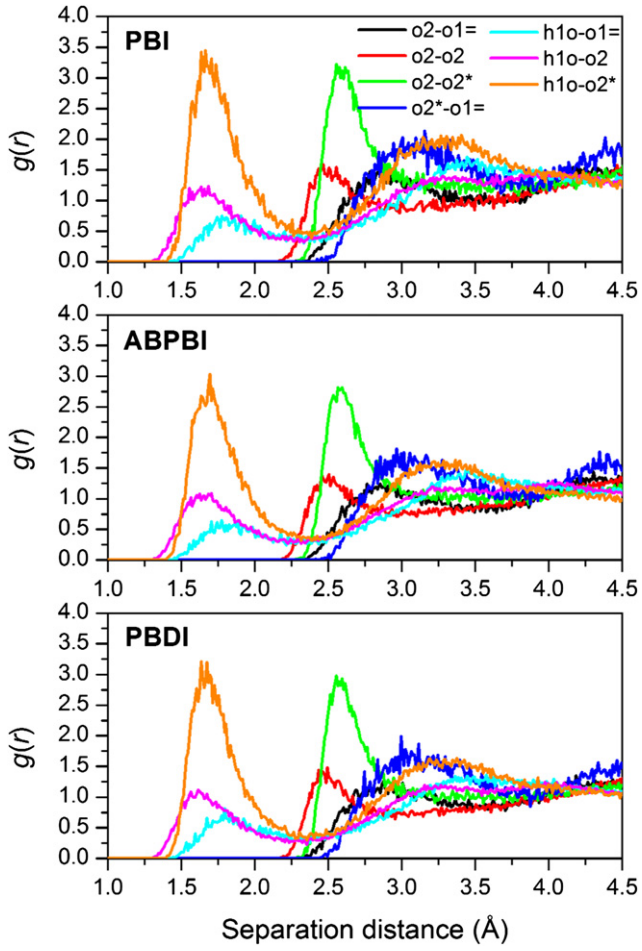

Fig. 6. RDF plots for intermolecular "o2–o1=", "o2–o2", "o2–o2*", "o2*–o1=", "h1o–o1=", "h1o–o2", and "h1o–o2*" atom pairs in PA-doped PBI, ABPBI, and PBDI.

3.4. Numbers of distinct hydrogen bonds

Quantities of distinct types of hydrogen bonds for three polybenzimidazoles under neat, hydrated, and PA-doped environments are illustrated in Figs. 8–11. For a better comparison between three polybenzimidazoles, the number of hydrogen bonds based on both imidazole unit and mass unit are calculated and presented.

Fig. 8 illustrates the quantities of the only hydrogen bond of "n3a-h1n ⋯ n2a" in neat polybenzimidazoles. As shown, there are 17.7, 20.8, and 15.6 hydrogen bonds per 100 imidazole moieties, which are 6.9, 10.8, and 8.1 hydrogen bonds per 10^{-20} g of neat PBI, ABPBI, and PBDI, respectively. ABPBI forms the largest number of hydrogen bonds no matter if the quantity is imidazole-averaged or mass-averaged. PBDI has the least imidazole-averaged hydrogen bonds which can be explained by the structure of its repeating unit. As shown in Fig. 1(c), the two imidazole rings in the PBDI repeating unit are closely connected by a phenyl ring. This may result in steric exclusion for simultaneous formation of multiple hydrogen bonds between parallel repeating units. The repeating unit of PBI has one more phenyl ring than that of PBDI, which decreases its mass-averaged number of hydrogen bonds.

Fig. 9(a) and (b) present the imidazole-averaged and mass-averaged quantities of distinct hydrogen bonds in hydrated polybenzimidazoles, respectively. As shown by Fig. 9(a), the imidazole-averaged quantities of "n3a–h1n ⋯ n2a" hydrogen bonds decreased to 10.1, 11.5, and 11.2 for PBI, ABPBI, and PBDI, respectively, when benzimidazole chains were mixed with water molecules. This explains why compressive strength and dynamic modulus of the PBI fibers in the wet state are reduced to half those of the dry materials [22]. Among all three types of hydrogen bonding, "o2*–h1o ⋯ n2a" has the largest quantities, which are 75.3, 82.8, and 86.1 for PBI, ABPBI, and PBDI, respectively. Quantities of "n3a–h1n ⋯ o2*" hydrogen bonds are the second, which are 45.6, 49.3, and 45.9 for PBI, ABPBI, and PBDI, respectively. These results agree well with the predicted strength order of these three hydrogen bonds by RDFs in Section 3.3: "o2*–h1o … n2a" (1.8 Å) > "n3a–h1n … o2*" (2.0 Å) and "n3a–h1n … n2a" (2.0 Å). The smaller number of "n3a–h1n … n2a" hydrogen bonds than that of "n3a–h1n … o2*" hydrogen bonds is probably due to constraints of the chain structure and the smaller number of available "n2a" acceptors compared to "o2*" acceptors (1:2).

Comparing three polybenzimidazoles, it can be noticed that PBI forms the fewest hydrogen bonds, especially for the strong hydrogen bonding of "o2*–h1o ⋯ n2a". This can also be due to the extra phenyl ring in its repeating unit, which makes PBI less hydrophilic and reduces the ability to form hydrogen bonding between the benzimidazole chain and water molecules. It also agrees with the experimental result that PBI has a lower water uptake than ABPBI [23,24]. For ABPBI and PBDI, the number of "n3a–h1n ⋯ o2*" hydrogen bonds for ABPBI is larger than that for PBDI by 3.4 and the number of "o2*–h1o ⋯ n2a" hydrogen bonds for ABPBI is smaller than that for PBDI by almost the same amount (3.3). Although the differences are small, ABPBI seems more prone to form hydrogen bonding of "n3a–h1n ⋯ o2*" and PBDI prefers "o2*–h1o ⋯ n2a". It also suggests ABPBI and PBDI should have similar water uptakes. Fig. 9(b) shows that the mass-averaged quantities of the three types of hydrogen

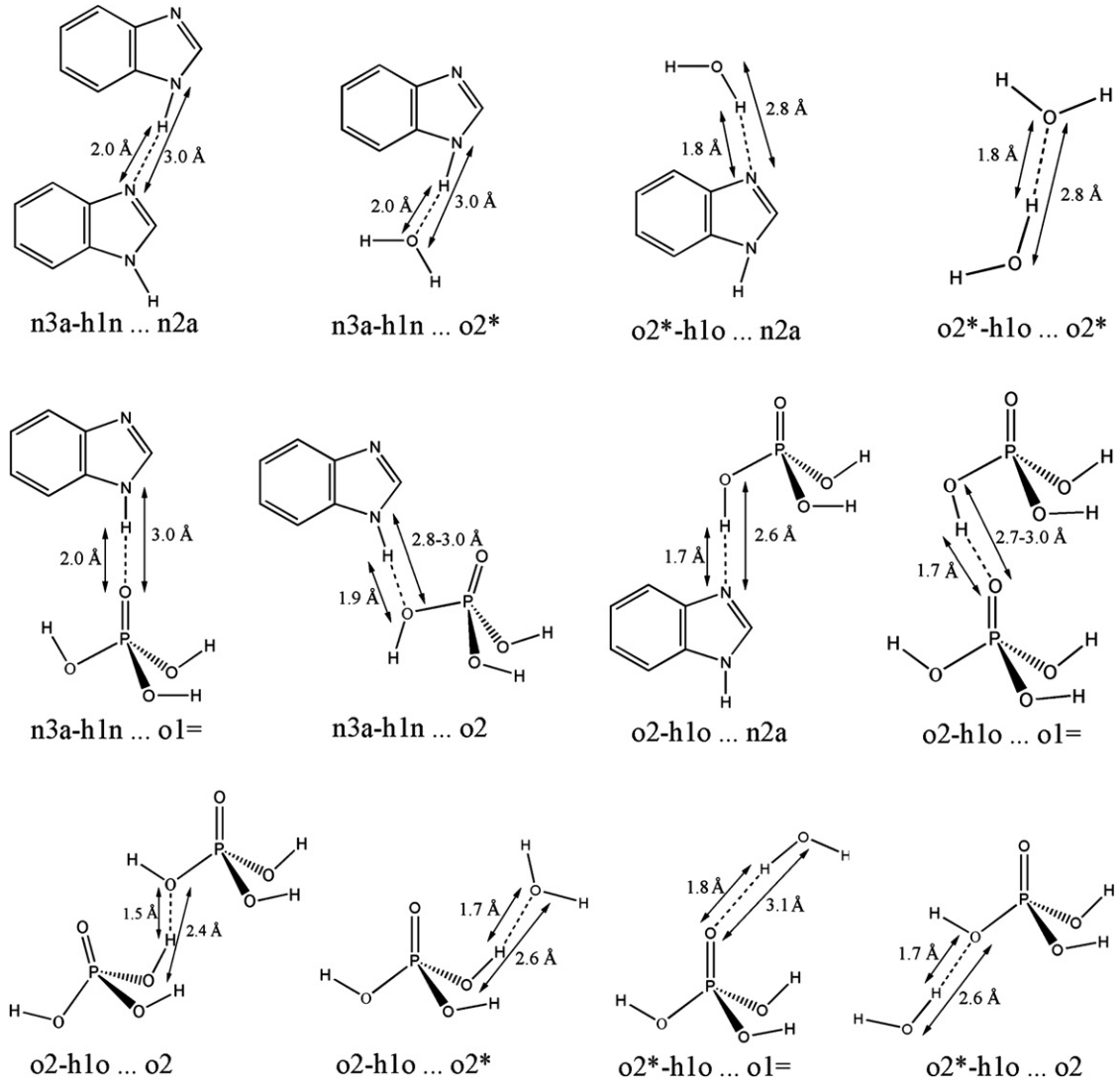

Fig. 7. Schematic representations of distinct types of hydrogen bonding in neat, hydrated, and PA-doped polybenzimidazoles.

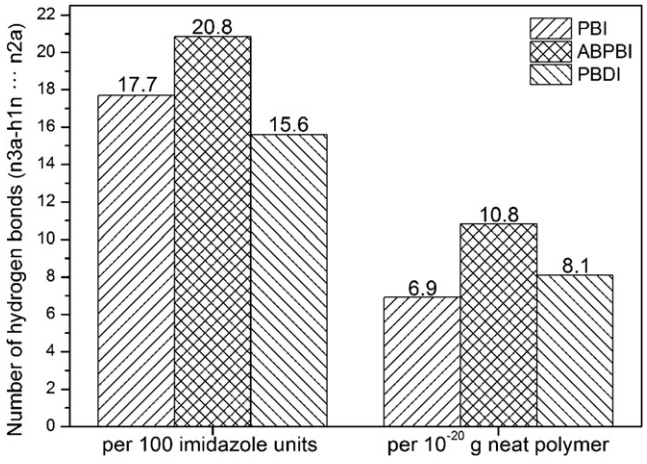

Fig. 8. Quantities of "n3a–h1n ··· n2a" hydrogen bonds per 100 imidazole moieties and per 10^{-20} g polymer in neat PBI, ABPBI, and PBDI.

bonds for PBI further decreased compared with ABPBI and PBDI. Detailed numbers can be read from the figure.

Fig. 10(a) and (b) show the imidazole-averaged and mass-averaged quantities of distinct polybenzimidazole-involved hydrogen bonds in PA-doped polybenzimidazoles, respectively. As shown by Fig. 10(a), the first three labels on the abscissa describe different types of hydrogen bonding between polybenzimidazole and PA. The fourth and the fifth labels are for hydrogen bonding between polybenzimidazole and water. The last one represents hydrogen bonding between different imidazole rings on the single benzimidazole chain. Between polybenzimidazole and PA, hydrogen bonds of "o2–h1o ··· n2a" are in the largest quantities, 43.3, 54.1, and 50.3 for PBI, ABPBI, and PBDI, respectively. They are closely followed by the numbers of "n3a–h1n ··· o2" hydrogen bonds, which are 36.8, 42.0, and 47.0 for PBI, ABPBI, and PBDI, respectively. The total number of "o2" atoms in the system is three times the number of "o1=" atoms, but hydrogen bonds of "n3a–h1n ··· o2" are more than four times as many as those of "n3a–h1n ··· o1=". From these results, it can be concluded with the strength order of the three hydrogen bonds: "o2–h1o ··· n2a" > "n3a–h1n ··· o2" > "n3a–h1n ··· o1=", which agrees well with RDF results in Section 3.3. In PA-doped polybenzimidazoles, hydrogen bonds of "o2*–h1o ··· n2a" between polybenzimidazole and water are also abundant, which are 35.7,

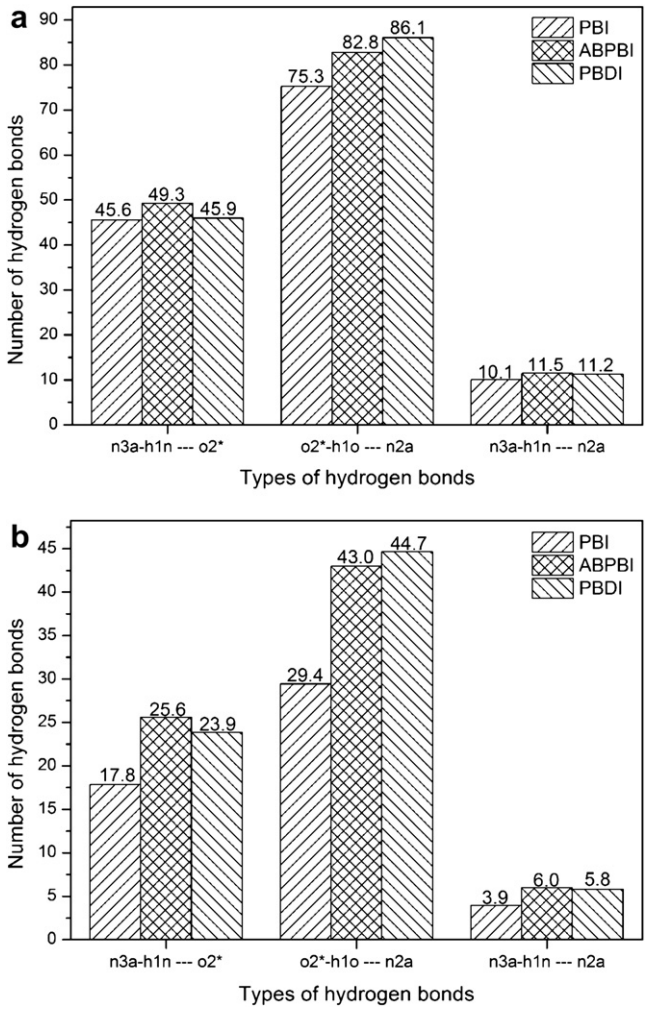

Fig. 9. (a). Quantities of "n3a–h1n ··· o2*", "o2*–h1o ··· n2a", and "n3a–h1n ··· n2a" hydrogen bonds per 100 imidazole moieties in hydrated PBI, ABPBI, and PBDI. (b). Quantities of "n3a–h1n ··· o2*", "o2*–h1o ··· n2a", and "n3a–h1n ··· n2a" hydrogen bonds per 10^{-20} g polymer in hydrated PBI, ABPBI, and PBDI.

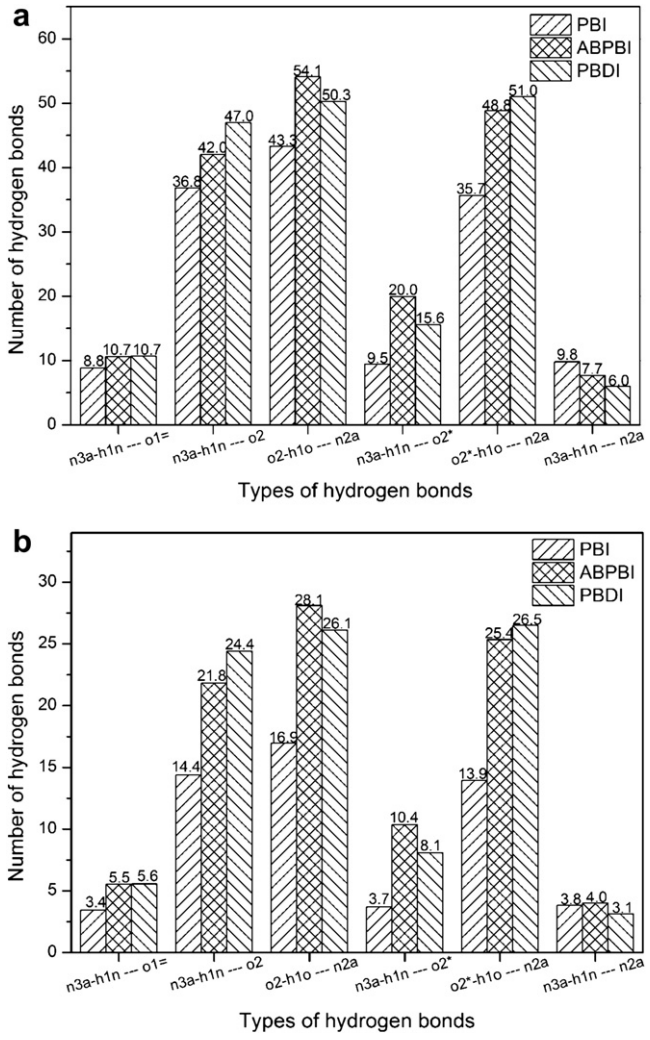

Fig. 10. (a). Quantities of "n3a–h1n ··· o1=", "n3a–h1n ··· o2", "o2–h1o ··· n2a", "n3a–h1n ··· o2*", "o2*–h1o ··· n2a", and "n3a–h1n ··· n2a" hydrogen bonds per 100 imidazole moieties in PA-doped PBI, ABPBI, and PBDI. (b). Quantities of "n3a–h1n ··· o1=", "n3a–h1n ··· o2", "o2–h1o ··· n2a", "n3a–h1n ··· o2*", "o2*–h1o ··· n2a", and "n3a–h1n ··· n2a" hydrogen bonds per 10^{-20} g polymer in PA-doped PBI, ABPBI, and PBDI.

48.8, and 51.0 for PBI, ABPBI, and PBDI, respectively. The numbers of "n3a–h1n ··· o2*" hydrogen bonds are 9.5, 20.0, and 15.6 for PBI, ABPBI, and PBDI, respectively, slightly larger than those of the "n3a–h1n ··· o1=" and "n3a–h1n ··· n2a" hydrogen bonds. These results indicate that "o2–h1o ··· n2a", "o2*–h1o ··· n2a", and "n3a–h1n ··· o2" are three primary hydrogen bonds among the six polybenzimidazole-involved hydrogen bonds in PA-doped systems. This also agrees reasonably well with the predicted strength order of hydrogen bonds from RDF results.

Among the three polybenzimidazoles, PBI forms the least number of hydrogen bonds except for "n3a–h1n ··· n2a". This can also be attributed to its less hydrophilic character and agrees with the experimental results that impregnation of ABPBI with a given PA solution leads to higher acid uptake in comparison with PBI [7,8]. Because less "N" sites are taken by PA and water molecules, the number of "n3a–h1n ··· n2a" hydrogen bonds (9.8) becomes slightly larger than that for ABPBI (7.7) and PBDI (6.0). For ABPBI and PBDI, the numbers of "n3a–h1n ··· o1=" hydrogen bonds are the same (10.7). The number of "n3a–h1n ··· o2" hydrogen bonds for ABPBI is smaller than that for PBDI by 5.0, and the number of "o2–h1o ··· n2a" hydrogen bonds for ABPBI is larger than that for PBDI by 3.8. Trends for the other three hydrogen bonds, "n3a–h1n ··· o2*", "o2*–h1o ··· n2a", and "n3a–h1n ··· n2a" are the same as those in hydrated ABPBI and PBDI. It can be concluded that, for the PA-doped systems, ABPBI also forms nearly the same total number of hydrogen bonds as PBDI (183.3 *vs.* 180.6). Fig. 10(b) presents the degree by which the extra phenyl ring in the RU of PBI can further decrease the mass-averaged quantities of hydrogen bonds. Detailed numbers can be read from the figure.

Fig. 11 presents the imidazole-averaged quantities of distinct hydrogen bonds between PA and water molecules in PA-doped PBI, ABPBI, and PBDI. The first two labels on the abscissa describe the two types of hydrogen bonding between PA molecules. The labels from the third through the fifth are for hydrogen bonding between PA and water molecules. The last one represents hydrogen bonding between water molecules. As shown, the differences between three polybenzimidazoles for all types of hydrogen bonding are unobvious. Therefore, only different types of hydrogen bonding are compared between each other, and the number of each type of hydrogen bonds is averaged over three polybenzimidazoles. Quantities of hydrogen bonds in descending order are: "o2–h1o ··· o2" (262.6) > "o2*–h1o ··· o2" (188.1) > "o2–h1o ··· o2*" (174.8) > "o2*–h1o ··· o2*" (124.6) > "o2–h1o ··· o1=" (67.2) > "o2*–h1o ··· o1=" (46.8). Results suggest that water should be directly involved in the conduction mechanism in PA-doped polybenzimazoles. Considering the number

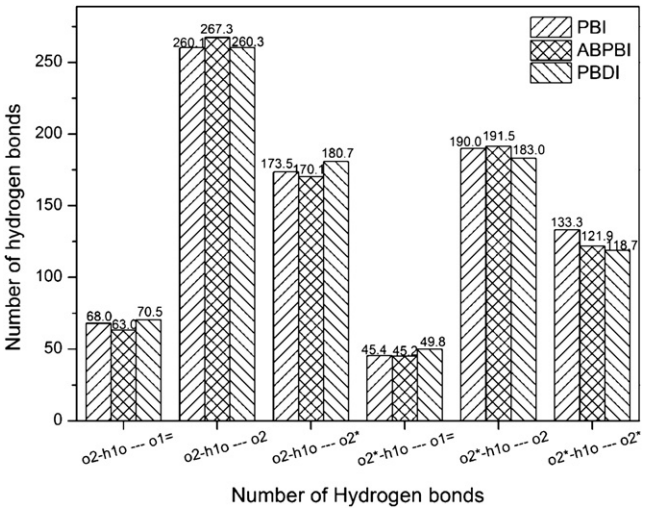

Fig. 11. Quantities of "o2–h1o ··· o1=", "o2–h1o ··· o2", "o2–h1o ··· o2*", "o2*–h1o ··· o1=", "o2*–h1o ··· o2", and "o2*–h1o ··· o2*" hydrogen bonds per 100 imidazole moieties in PA-doped PBI, ABPBI, and PBDI.

ratios of "o2" atoms to "o1=" atoms to "o2*" atoms in the systems are 3:1:1, these hydrogen bond results also agree reasonably with the RDF conclusions made in Section 3.3. Comparing Figs. 10(a) and 11, the total number of hydrogen bonds between PA and water molecules (864.1) is nearly five times as many as the polybenzimidazole-involved number of hydrogen bonds (*e.g.* 180.6 for ABPBI). Therefore, proton transfers will mainly occur between PA and water molecules in the proposed PA-doped polybenzimidazole models.

4. Conclusions

As the results indicate, the COMPASS force field has been successful in reproducing densities and WAXD patterns of neat and PA-doped polybenzimidazoles. RDFs were used to estimate lengths of distinct types of hydrogen bonds and distances between hydrogen donor and acceptor atoms. By comparing lengths of hydrogen bonds, conclusions were made that the strength of hydrogen bonding is mainly determined by the donor and indicate an order of decreasing donor strength as "PA > water > polybenzimidazole". In the case that donors are the same, the hydroxyl oxygen atom in PA acting as acceptor forms the strongest hydrogen bond compared to other types of hydrogen acceptors. Results on quantities of distinct types of hydrogen bonds confirmed the RDF conclusions. In addition, all three polybenzimidazoles show nearly the same WAXD patterns and RDF plots. The less hydrophilic character of PBI and its lower affinity towards PA compared with either ABPBI or PBDI has been confirmed by density results and quantities of distinct hydrogen bonds. In a subsequent communication, the effect of water concentration, PA-doping level, and temperature on hydrogen bonding in the ABPBI system will be reported.

Acknowledgment

Acknowledgment is made to the donors of the American Chemical Society Petroleum Research Fund (ACS PRF # 45666-AC5) and National Science Foundation (NSF) Research Experiences for Undergraduates (REU) Site Program in Membrane Applied Science and Technology (EEC Award #0139438) for financial support of this research.

Appendix. Supplementary data

Supplementary data associated with this article can be found in the online version, at doi:10.1016/j.polymer.2010.09.021.

References

[1] Buckley A, Stuetz DE, Serad GA. Polybenzimidazoles. In: Mark HF, editor. Encyclopedia of polymer science and engineering. New York: John Wiley & Sons; 1988. p. 572–601.
[2] Welsh WJ. Poly(benzimidazole). In: Mark JE, editor. Polymer data handbook. New York: Oxford University Press; 1999. p. 288–90.
[3] Wainright JS, Wang JT, Wang D, Savinell R, Litt M. J Electrochem Soc 1995;142 (7):L121–3.
[4] Costamagna P, Srinivasan S. J Power Sources 2001;102(1):242–52.
[5] Kreuer KD, Paddison SJ, Spohr E, Schuster M. Chem Rev 2004;104(10):4637–78.
[6] Asensio JA, Gomez-Romero P. Fuel Cells 2005;5(3):336–43.
[7] Asensio JA, Sánchez EM, Gómez-Romero P. Chem Soc Rev 2010;39 (8):3210–39.
[8] Mader J, Xiao L, Schmidt TJ, Benicewicz BC. Adv Polym Sci 2008;216:63–124.
[9] Li Q, Jensen JO, Savinell RF, Bjerrum NJ. Progress in Polymer Science 2009;34 (5):449–77.
[10] Li Q, He R, Gao JA, Jensen JO, Bjerrum NJ. J Electrochem Soc 2003;150:A1599.
[11] Krishnan P, Park JS, Kim CS. J Power Sources 2006;159(2):817–23.
[12] Inoue S, Imai Y, Uno K, Iwakura Y. Die Makromolekulare Chemie 1966;95: 236–47.
[13] Cho J, Blackwell J, Chvalun SN, Litt M, Wang Y. J Polym Sci, Part B: Polym Phys 2004;42(13):2576–85.
[14] Wereta Jr A, Gehatia MT, Wiff DR. Polym Eng Sci 2004;18(3):204–9.
[15] Krause SJ, Haddock T, Price GE, Lenhert PG, O'Brien JF, Helminiak TE, et al. J Polym Sci, Part B: Polym Phys 2003;24(9):1991–2016.
[16] Akbey U, Graf R, Chu PP, Spiess HW. Aust J Chem 2009;62(8):848–56.
[17] Carollo A, Quartarone E, Tomasi C, Mustarelli P, Belotti F, Magistris A, et al. J Power Sources 2006;160(1):175–80.
[18] Litt M, Ameri R, Wang Y, Savinell R, Wainwright J. Mater Res Soc Symp Proc 1999;548:313–24.
[19] Staiti P, Lufrano F, Aricņ A, Passalacqua E, Antonucci V. J Membr Sci 2001;188 (1):71–8.
[20] Asensio JA, Borrós S, Gómez-Romero P. J Electrochem Soc 2004;151:A304.
[21] Asensio JA, Borrós S, Gómez-Romero P. J Membr Sci 2004;241(1):89–93.
[22] Brooks NW, Duckett RA, Rose J, Ward IM, Clements J. Polymer 1993;34 (19):4038–42.
[23] Li Q, He R, Berg RW, Hjuler HA, Bjerrum NJ. Solid State Ionics 2004;168 (1–2):177–85.
[24] Diaz LA, Abuin GC, Corti HR. J Power Sources 2009;188(1):45–50.
[25] Tomlin DW, Fratini AV, Hunsaker M, Wade Adams W. Polymer 2000;41 (25):9003–10.
[26] Ma YL, Wainright JS, Litt MH, Savinell RF. J Electrochem Soc 2004;151:A8.
[27] Sun H. J Phys Chem B 1998;102(38):7338–64.
[28] Sun H, Ren P, Fried JR. Comput Theor Polym Sci 1998;8(1–2):229–46.
[29] Material studio 5.0. San Diego: Accelrys Software Inc.; 2009.
[30] Lifson S, Hagler AT, Dauber P. J Am Chem Soc 1979;101(18):5111–21.
[31] Sun H, Mumby SJ, Maple JR, Hagler AT. J Phys Chem 1995;99(16):5873–82.
[32] Will G. Z Kristallogr 1969;129:211–21.
[33] Dik-Edixhouven C, Schenk H, van der Meer H. Crystal Struct Commun 1973;2:23–4.
[34] Andersen HC. J Chem Phys 1980;72:2384–93.
[35] Berendsen HJC, Postma JPM, van Gunsteren WF, DiNola A, Haak JR. J Chem Phys 1984;81:3684.
[36] Ewald PP. Ann Phys (Leipzig) 1921;64:253.
[37] Powers EJ, Serad GA. History and development of polybenzimidazoles. In: Seymour RB, Kirschenbaum GS, editors. High performance polymers: their origin and development. Amsterdam: Elsevier; 1986. p. 355.
[38] Hwang WF, Wiff DR, Verschoore C, Price GE, Helminiak TE, Adams WW. Polym Eng Sci 2004;23(14):784–8.
[39] Hughes CE, Haufe S, Angerstein B, Kalim R, Mahr U, Reiche A, et al. J Phys Chem B 2004;108(36):13626–31.
[40] Soper AK, Phillips MG. Chem Phys 1986;107(1):47–60.
[41] Mark P, Nilsson L. J Phys Chem A 2001;105(43):9954–60.
[42] Li S, Fried JR, Sauer J, Colebrook J, Dudis DS. Int J Quantum Chem, in press. doi:10.1002/qua.22702.